ISIJ International, Vol. 45 (2005), No. 7, pp. 1001–1004

Phenomenological Discussion of Fe and Co Film Electrodeposited in a Magnetic Field

H. MATSUSHIMA, Y. FUKUNAKA, H. YASUDA[1)] and S. KIKUCHI[2)]

Graduate School of Energy Science, Kyoto University, Sakyo-ku, Kyoto 606-8501 Japan. E-mail: fukunaka@energy.kyoto-u.ac.jp
1) Graduate School of Engineering, Osaka University, Yamada-oka, Osaka 565-0871 Japan.
2) Department of Materials Science, The University of Shiga Prefecture, Hatsusaka-cho, Hikone, Shiga 522-0057 Japan.

(*Received on February 28, 2005; accepted on April 12, 2005*)

Fe and Co films were galvanostatically electrodeposited at 10 mA cm^{-2} on Cu substrate in sulfate aqueous solution with pH=1.5. The amount of electricity of 150 C cm^{-2} was selected. The magnetic field (0–5 T) was superimposed parallel to the electrode plane. The superimposition of magnetic field to the electrodeposition process considerably decreased the current efficiency with increasing in the magnetic flux for Fe, while almost constant efficiency was maintained for Co. SEM images showed the smoother surface morphology of Fe film. Texture measurement demonstrated that Fe(110) plane was oriented to the magnetic field direction. On the other hand, the surface morphology of Co deposits was drastically changed from an angular to a platelike shape by superimposing the magnetic field. Comparing with the case of Fe texture evolution, Co texture variation with magnetic flux was not evident. The magnetohydrodynamic (MHD) effects on Fe and Co electrodeposited films are phenomenologically discussed.

KEY WORDS: iron and cobalt electrodeposition; magnetic field; surface morphology; texture; MHD convection.

1. Introduction

Electrodeposition is one of the convenient and established techniques that can control the surface morphology and the crystal orientation of thin films as well known.[1,2)] The application to the "perpendicular" magnetic recording media[3)] and giant magnetoresistance (GMR)[4)] may provide a good opportunity for the electrochemical processing to be further advanced. In order to tailor the unique microstructural interface, the introduction of another degree of freedom of magnetic field to the electrochemical reaction field may be promising. A number of research groups have reported some unique phenomena during electrodeposition in a magnetic field.[5–15)]

When an electrodeposition is conducted in a magnetic field, the magnetohydrodynamic (MHD) convection is induced by Lorenz force. Devos *et al*.[16)] reported that the surface morphology of electrodeposited Ni film was smoothed and the preferred orientation was drastically changed from (200) in 0 T to (220) in 5 T. These phenomena were explained by MHD convection that enhanced the mass transfer of organic additives near the electrode surface.

Magnetocrystalline anisotropy is considered to be another effect on surface microstructure, which is caused by the anisotropic magnetization energy for different crystallographic axis. Bodea *et al*.[17)] reported that the macroscopic morphology of Fe dendrite remarkably changed from circular shape in 0 T to rectangular in 0.2 T. It was understood by minimizing magnetic dipolar energy of growing branches. Monte Carlo simulation by Li *et al*.[15)] showed that the crystal orientation could be determined by the crystallographic factors like surface energy anisotropy and magnetocrystalline anisotropy.

The high magnetic field effects on the microstructure of electrodeposited thin film have been also examined in Kyoto University. The present paper describes the phenomenological discussion about the magnetic field effect on surface morphology and pole figure variation of electrodeposited Fe and Co film.

2. Experimental

Electrochemical experiments were carried out with a three-electrode system as illustrated in **Fig. 1**. The duct type electrode assembly was composed of a short rectangular channel (10 mm×10 mm×30 mm, polystyrene) with two open ends. It was immersed in 300 mL electrolytic bath. Cu sheet (10 mm×10 mm×0.2 mm, Cu 99.99%, Nilaco Corp.) was used as the cathode. Fe or Co sheet with the same surface area as the Cu cathode was used as the anode. They were embedded in either side of channel walls. Before starting the electrodeposition, Cu cathode was electropolished in 70 wt% H_3PO_4 acid solution for 1 h with a terminal voltage of 1.3 V. It was then rinsed with distilled water and dried by Ar gas. A reference electrode was an Ag/AgCl electrode with a saturated KCl aqueous solution.

An electrolyte composition was 0.90 mol $FeSO_4$ L^{-1} or 0.90 mol $CoSO_4$ L^{-1}. The pH of electrolyte solution was adjusted to 1.5 with H_2SO_4. It was deaerated by bubbling Ar gas for more than an hour. The solution temperature was

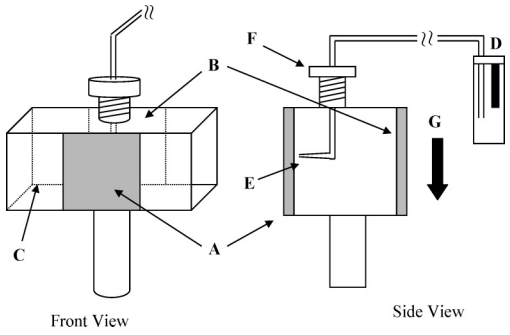

Fig. 1. Schematic illustration of the electrode assembly. A: cathode (Cu, 1 cm^2), B: anode (Fe, 1 cm^2), C: duct channel (10 mm×10 mm×30 mm), D: reference (Ag/AgCl), E: luggin probe, F: plastic screw, G: gravitational direction, H and H': magnetic field direction.

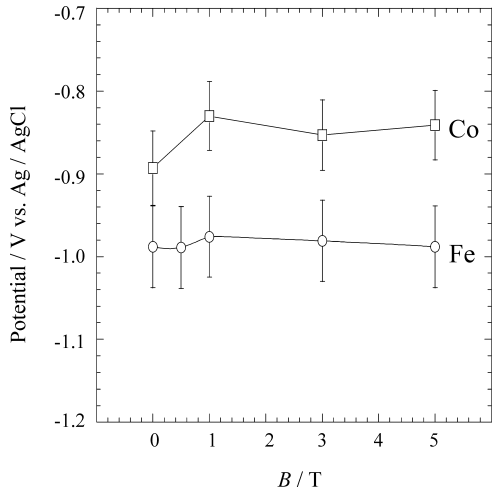

Fig. 2. Steady state electrode potential variation of Fe (○) and Co (□) with magnetic flux densities at 10 mA cm^{-2}.

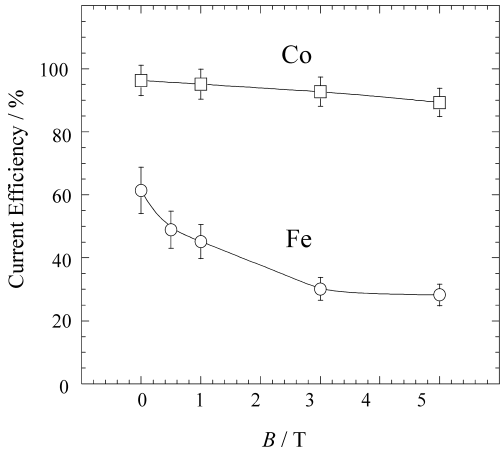

Fig. 3. Dependence of Fe (○) and Co (□) current efficiency on magnetic flux densities.

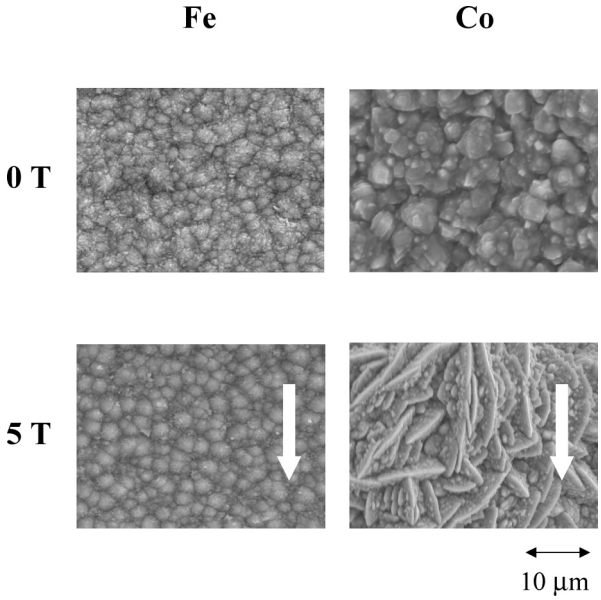

Fig. 4. Surface morphology comparison of Fe and Co electrodeposited in 0 T and 5 T. (An arrow shows direction of magnetic field.)

maintained at 298 K.

Electrodeposition was galvanostatically conducted at 10 mA cm^{-2} until the amount of electrical charge reached 150 C cm^{-2}. The electrolysis was carried out in a static and uniform magnetic field which was superimposed parallel to the electrode plane. The magnetic field up to 5 T was generated by a superconducting magnet (CSM-6T, Sumitomo Heavy Industries Co. Ltd.).

The electrodeposited film was weighted in order to estimate current efficiency for Fe or Co electrodeposition. The surface morphology was observed by SEM (S-2600H, Hitachi). The crystal structure was analyzed by XRD (X'Pert, Philips, Cu-Kα line, 50 kV, 40 mA).

3. Results

3.1. Fe Electrodeposition

When the electrolytic circuit was closed, the electrode potential shifted in the negative direction from the rest potential and attained a steady value after a few minutes. **Figure 2** shows the dependence of a steady state electrode potential on the magnetic flux densities. Standard deviation was calculated to be about 50 mV from five independent measurements. The deposition potential is kept constant around −0.99 V *vs.* Ag/AgCl reference in any magnetic field intensities. No significant influence due to magnetic flux on the electrode potential was noticed.

Hydrogen gas bubbles simultaneously evolved during Fe electrodeposition. The equilibrium electrode potential of H^+/H_2 couple is −0.31 V in this electrolyte solution (pH= 1.5) and that of Fe^{2+}/Fe is −0.66 V *vs.* Ag/AgCl. It is believed that the hydrogen overpotential on Fe electrode is over 300 mV.[18] Thus, the electrode potential recorded in Fig. 2 exceeds by 380 mV over such hydrogen overpotential. The significant evolution rate of H_2 gas is thus expected from the current efficient of 60% as seen in **Fig. 3**. The superimposition of magnetic field induces macroscopic MHD convection to supply the bulk fresh electrolyte to the cathode surface installed in the duct type cell. Then, the current efficiency starts to further decrease from 62% in 0 T to 30% in 5 T with increasing in the magnetic flux density.

Figure 4 shows SEM images of Fe film electrodeposited in (a) 0 T and (b) 5 T. The film thickness varies from 70 to 20 μm depending on the magnetic flux density. Figure 4(a) (B=0 T) demonstrates that the surface morphology consists

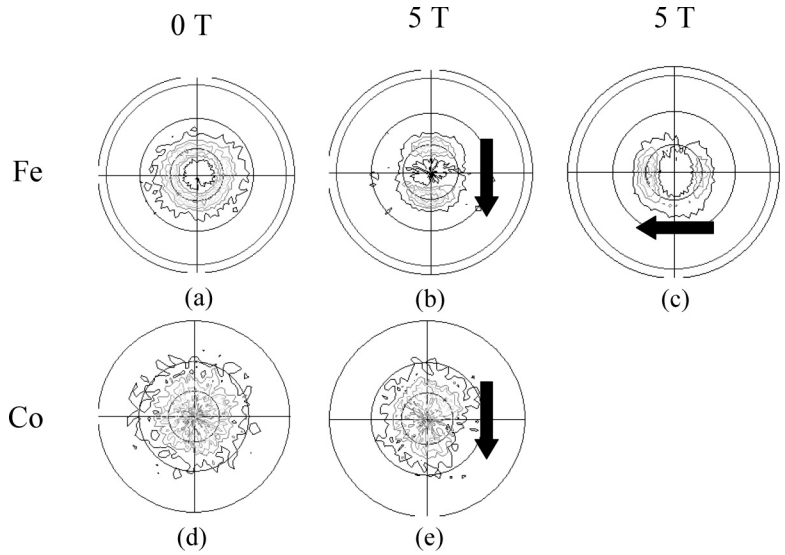

Fig. 5. Pole figures of Fe(110) plane and Co(002) plane electrodeposited at 10 mA cm^{-2}. (An arrow shows direction of magnetic field.)

of angular shape of Fe grains. The size distribution of Fe precipitates is rather broad. Figure 4(b) (B=5 T) shows much smoother surface morphology in the magnetic field.The shape of Fe precipitate is roundish and the size distribution becomes narrower.

X-ray pole figure was measured in order to investigate the magnetic field effect on crystal texture. Pole figure variation of Fe(110) plane with magnetic field is illustrated in **Fig. 5**. Sample (a) corresponds to the pattern without magnetic field, while samples (b) and (c) do to those in a magnetic field of 5 T, respectively. The direction of magnetic field was applied orthogonally each other with maintaining the parallel direction to the electrode surface. Figure 5(a) shows an annular symmetric pattern at the angle of about 30 degrees to the direction normal to the substrate plane. On the other hand, Figs. 5(b) and 5(c) demonstrate the anisotropic characteristics governed by the magnetic field vector orthogonally superimposed each other. They clearly respond with the rotation of magnetic field vector.

3.2. Co Electrodeposition

Co film was electrodeposited under a similar electrolysis condition to the case of Fe. Figure 2 shows the dependence of electrodeposition potential of Co on magnetic flux density. The standard deviation of 40 mV may be still too large to mention that the electrode potential for Co deposition is shifted to positive direction by superimposing the magnetic field. However, the dependence for Co is slightly larger than the case for Fe.

The equilibrium electrode potential for Co^{2+}/Co reaction is about −0.4 V *vs.* Ag/AgCl reference. The electrode potential was measured about 100 to 160 mV to more noble direction than the case of Fe. The measured degree exceeding the hydrogen overpotential thus decreases to about 220 to 280 mV, when the same value of hydrogen gas evolution overpotential is assumed on Co substrate. It is compared with 380 mV for Fe case. Thus, the current efficiency must be considerably improved as seen in Fig. 3. Because the partial current density consumed to H_2 gas evolution is small, the surface composition variation becomes smaller even under MHD convection.

SEM images of Co film electrodeposited in (a) 0 T and (b) 5 T are shown in Fig. 4. In the absence of magnetic field, the morphology of Co precipitates is irregular in shape. The grain size is estimated to be about 1 μm that is much larger than that of Fe precipitates. The superimposition of magnetic field results in the drastic morphological variation in Co film. A platelike structure is preferentially grown in Fig 4.

Figure 5 shows the pole figure of (002) plane of Co film electrodeposited in (d) 0 T and (e) 5 T. A circle pattern at the angle of 30 degrees normal to the electrode surface appears in 0 T (d). Comparing with the Fe pattern in Fig. 5 (a), it is broadly distributed. On the other hand, the superimposition of 5 T induces an anisotropic pattern along the same direction as the magnetic field vector (e).

4. Discussion

When a transition metal film is electrodeposited in magnetic field, the film microstructure may be characterized by two factors, (1) crystallographic magnetic anisotropy and (2) MHD convection.

As far as the first factor concerns, the results of texture analysis indicated that the easy magnetization plane, Fe(100) and Co(002), was not oriented to the magnetic field direction. The anisotropic texture evolution shown in Fig. 5 cannot be explained by the crystallographic magnetic anisotropy, thus, the possibility due to the first factor is discarded.

When MHD convection effect on the morphology and microstructural variation is focused, the duplex phenomena must be discussed, which are caused by both macroscopic and microscopic MHD convection. The superimposition of magnetic field introduces the remarkable differences in the current efficiency between Fe and Co electrodeposition. It is attributed to the essential overpotential to the significant H_2 gas evolution rate of H^+/H_2 reaction (HER). The standard electrode potential of Fe^{2+}/Fe couple is −0.44 V *vs.* HER, which is less noble than that of Co^{2+}/Co couple

(−0.28 V *vs.* HER). Hydrogen overpotential as the kinetic resistance to introduce the significant H_2 gas bubble evolution on the substrate surface must be taken into account as well as the standard electrode potential. H_2 gas overpotential has been measured frequently on various transition metal cathodes. It is believed over 300 mV. It is further assumed that there is no difference between H_2 overpotential on Fe and Co. That is, H_2 gas evolution rate accompanied with Fe^{2+}/Fe reduction is much faster than the case for Co^{2+}/Co reduction.

Under the conventional electrodeposition of Fe ($B=0$ T), the pH value near cathode surface significantly increases because H^+ is consumed by HER. It introduces the less noble electrode potential for H_2 gas evolution which results in high current efficiency for Fe deposition. On the other hand, macroscopic MHD convection enhances the ionic mass transfer of H^+ and Fe^{2+} ions during Fe electrodeposition in a magnetic field. The cathode surface pH variation closely related to the hydroxide and the oxide formation determines the crystal growth mechanism.[19–21] That is, "Macro-MHD" convection changes the concentration profiles of H^+ and Fe^{2+} in the concentration boundary layer. Moreover, the hydroxides formation might induce an anisotropic texture evolution as shown in Fig. 5. In the case of Co electrodeposition, the variation of pH must be smaller. The adsorption species such as hydroxide and oxide is hardly produced, resulting in ambiguous texture pattern shown in Fig. 5

Surface roughness of electrodeposited film must be considerably improved by macroscopic MHD convection. It is essentially related to the mass transfer rate inside a concentration boundary layer thickness formed near the cathode. Since an electric force line easily focuses on the tip of electrodeposits, it curves near the edge of precipitate to sometimes enhance an extraordinary growth process. Similar effect may be anticipated near the gas bubble evolving inside the concentration boundary layer. When the magnetic field couples with the bended electric force line, the complex microscopic convection, "Micro-MHD", is generated.

In the case of Fe electrodeposition, evolving gas bubbles are uniformly moving or rolling on the vertical plane electrode surface by both natural and macroscopic MHD convections. The bubbles motion temporally breaks the distortion of the electric force line. Therefore, the effects of micro-MHD may be masked by the continuous gas evolution, resulting in a rather uniform morphological variation.

On the other hand, H_2 gas evolution hardly occurs during Co electrodeposition. Since the coupling between magnetic and electric field is maintained larger than the case of Fe, micro-MHD convection effect may appear. Further examination to extract the micro-MHD convection inside a macroscopic concentration boundary layer is indispensable.

5. Conclusions

The comparison of Fe and Co electrodeposition in the magnetic field (0–5 T) was conducted by measuring the variations in current efficiency, surface morphology and crystal structure with the electrochemical processing parameters. The superimposition of magnetic field remarkably decreased the Fe current efficiency from 62% in 0 T to 30% in 5 T, while that for Co was constant above 90%. The pole figure measurement shows the (110) texture oriented to the magnetic field direction.

In the case of Co electrodeposition, the superimposition of magnetic field induced a significant surface morphological transition from granular to unique platelike structure erected vertically to the electrode plane. These variations might be caused by macroscopic and microscopic MHD convection that enhanced the ionic mass transfer to change the surface pH value at the cathode.

Acknowledgments

This study was partly supported by 21st COE program (Establishment of COE on Sustainable-Energy System) and the Ministry of Education, Science and Culture (Grant-in-Aid for Exploration Research No. 15360402), for which the authors are grateful.

REFERENCES

1) E. Budevski, G. Staikov and W. J. Lorenz: Electrochemical Phase Formation and Growth, VHC Publisher, Weinheim, (1996), 263.
2) H. D. Merchant: Defect Structure, Morphology and Properties of Deposits, TMS Publisher, Pennsylvania, (1995), 115.
3) M. Zheng, G. Choe and K. E. Johnson: *J. Appl. Phys.*, **91** (2002), 7068.
4) M. Uhlemann, A. Gebert, M. Herrich, A. Krause and L. Shultz: *Electrochim. Acta*, **48** (2003), 3005.
5) T. Z. Fahidy: *Prog. Surf. Sci.*, **68** (2001), 155.
6) J. M. D. Coey, G. Hinds, C. O'Reilly and T. R. Mhiochain: *Mater. Sci. Forum*, **373** (2001), 1.
7) A. Bund and A. Ispas: *J. Electroanal. Chem.*, **575** (2005), 221.
8) H. Matsushima, T. Nohira and Y Ito: *Electrochem. Solid State Lett.*, **7** (2004), C81.
9) H. Matsushima, T. Nohira, I. Mogi and Y. Ito: *Surf. Coat. Technol.*, **179** (2004), 245.
10) I. Tabakovic, S. Riemer, V. Vas'ko, V. Sapozhnikov and M. Kief: *J. Electrochem. Soc.*, **150** (2003), C635.
11) T. Sugiyama, M. Tahashi, K. Sassa and S. Asai: *ISIJ Int.*, **43** (2003), 855.
12) K. H. Lee, J. Yoo, J. Ko, H. Kim, H. Chung, D. Chang and J. Y. Lee: *Physica C*, **372** (2002), 866.
13) C. O'Reilly, G. Hinds and J. M. D. Coey: *J. Electrochem. Soc.*, **148** (2001), C674.
14) R. N. O'Brien and K. S. V. Santhanam: *J. Appl. Electrochem.*, **27** (1997), 573.
15) D. Y. Li and J. A. Szpunar: *Electrochim. Acta*, **42** (1997), 37.
16) O. Devos, A. Olivier, J. P. Chopart, O. Aaboubi and G. Maurin: *J. Electrochem. Soc.*, **145** (1998), 401.
17) S. Bodea, L. Vignon, R. Ballou and P. Molho: *Phys. Rev. Lett.*, **83** (1999), 2612.
18) H. Kita: *J. Electrochem. Soc.*, **113** (1966), 1095.
19) Y. Fukunaka, H. Doi and Y. Kondo: *J. Electrochem. Soc.*, **137** (1990), 88.
20) A. Bund, S. Koehler, H. H. Kuehnlein and W. Plieth: *Electrochim. Acta*, **49** (2003), 147.
21) A. Krause, M. Uhlemann, A. Gebert and L. Shultz: *Electrochim. Acta*, **49** (2004), 4127.